International Journal of Control and Automation
Vol. 9, No. 11 (2016), pp.327-342
http//dx.doi.org/10.14257/ijca.2016.9.11.28

Looper-Tension Control for Hot Strip Finishing Mills Based On the Combination of H∞ and ISMC Approaches

Zhaozhun Zhong[1], Jingcheng Wang[2] and Binna Song[1*]

[1]*School of Iron and Steel, Soochow University, Suzhou 215021, Jiangsu, PR China*
[2]*Department of Automation, Shanghai Jiaotong University, Shanghai 200240, PR China*
[*]*nustzzz@163.com*

Abstract

The development of an innovative controller for looper and tension control in hot strip finishing mills is traced based on the combination of H∞ and ISMC (integral sliding mode control) approaches. First, an H∞ controller is designed to robustly attenuate the unmatched disturbances in the angle and tension loops. Then, ISMC is used to overcome the matched disturbances in the actuators which guarantees the reliability and performances of the overall system. This solution has been considered thanks to its well-known robustness and simplicity characteristics concerning disturbances and unmodeled dynamics. Simulation results show the effectiveness of the proposed controller compared with conventional ones.

Keywords: *Looper-tension control; integral sliding mode control; H∞ control; hot strip finishing mills*

1. Introduction

This paper considers the control issues in hot strip mills of the iron and steel industry. The role of a hot strip mill process is to roll the slabs into strips. To be specific, during the casting process, a continuous steel slab (typically 250mm thick) is made, and cut into bars (about 10m long). The bars are then reheated up to the optimal temperature (around 1240 °C) in a furnace and then rolled on the reversing roughing mills by making several passes (forward and reverse). At the end of this roughing process, the steel pieces are typically 30-35mm thick (about 70m long) and their temperatures will be about 1050 °C . After the roughing process, the strips pass through the crop shear before entering the six or seven close coupled finishing mills [1]. The objective of hot strip finishing mills is to make further reduction of thickness and produce strips up to 0.8-20mm thick which are cooled down on run-out tables, and finally, coiled at the down coiler. The throughput of a modern hot strip mill is quite impressive: 5 million tunes per year. With such a high throughput, expensive mechanical equipments and modern control strategies are necessary in the process [2].

As for the product, the major specifications which should be satisfied are mechanical properties, surface and dimensional quality, and stable mill operation. As far as the control problem is concerned, the dimensional quality is controlled mainly by dedicated control systems such as AGC (automatic gauge control), AWC (automatic width control) and ASC (automatic shape control). On the other hand, stable mill operation through smooth threading of the strip is achieved by mass flow control which is used to balance the input and output flow of a strip in a stand. Each rolling stand is driven by a main motor which controls speed from ASR (automatic speed regulator). It was experienced that, during strip threading, strip tension is critical to strip quality and stable operation of the process

ISSN: 2005-4297 IJCA

[3]. Therefore between each pair of rolling stands, it is equipped with a looper system, shown in Figure 1, which is used to maintain upward pressure on the strip and keep the strip tension at a desired value during operation. The looper arm movement provides variation in strip storage length between the two stands to relax the mass flow unbalance and fluctuations. So the looper angle should be kept at a desired constant value for giving the system some leeway to absorb abnormal large changes in looper length. Therefore, looper and tension control is the key to the strip quality and successful mill operations.

There are several factors, such as significant parameter uncertainties, disturbances and nonlinear nature of the system, make looper and tension control design challenging. For the last three decades, many control schemes, such as conventional PI, decoupling, H∞, ILQ and so on [4, 5], have been proposed in the looper and tension control system. Recently, in order to overcome the disturbances and unmodelled dynamics, a robust technique: SMC (sliding mode control), is adopted in [6] to design an innovative friction compensation controller. In the literature, SMC is well-known for its robustness withstand matched disturbances and simplicity characteristics concerning industrial applications [7, 8]. However, the conventional SMC also has some disadvantages: the lack of robustness against unmatched disturbances, the reaching phase and so on. Many scholars have focused their researches on the designing of SMC systems with mismatched perturbations [9]. One of those methods is ISMC which is proposed as a way to combine the use of SMC with that of so-called "high level controller" [10, 11]. The high level controller (H∞ controller [12]) is designed to robustly stabilize the nominal system with unmatched disturbances, while ISMC rejects the matched disturbances. By this specific combination, we may expect better performances of the overall system.

As it will be shown in Section 2, the looper and tension system is subjected to both matched and unmatched disturbances. Since conventional SMC technique might not be quite adequate in this case, we aim to develop a H∞ disturbance attenuation controller based on ISMC. To be specific, H∞ controller is designed to robustly attenuate the unmatched disturbance, while ISMC guarantees the performance of H∞ controller in spite of the matched disturbances. And more details will be discussed in Sections 3 and 4.

The paper is organized as follows: The process model is described in Section 2, and the review of ISMC and H∞ technique is given in Section 3. Then, looper and tension control architecture is discussed in Section 4, simulation results and conclusions are shown in Sections 5 and 6 respectively.

2. Process Model

In this section, we give an overview of the looper and tension model which is used to synthesize the controllers. The model description follows closely that in [1], and forms the background of the control problem. The looper and interstand geometry is given in Figure 1 and the nomenclature is given in Table 1.

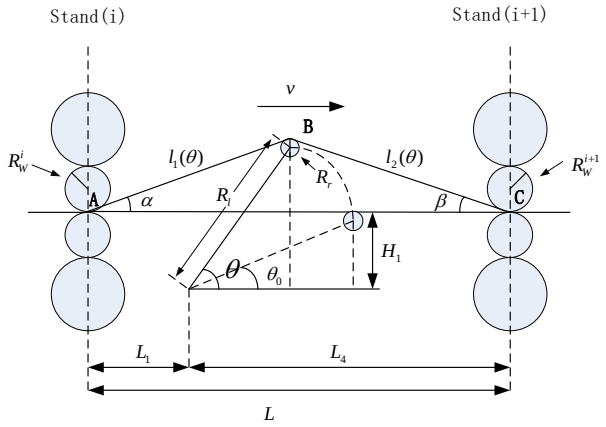

Figure 1. Looper and Interstand Geometry

2.1. Looper Dynamics

Apply Newton's law of motion to the looper system, we get:

$$J\ddot{\theta}(t) = T_u(t) - T_{load}(\theta) + w_\omega(t) \tag{1}$$

where J is the total inertia of the looper with respect to the pivoting point, $T_u(t)$ denotes the actuator torque on the looper, $T_{load}(\theta)$ represents the load torque on the looper and $w_\omega(t)$ denotes the unmodeled dynamics. $T_{load}(\theta)$ is the combination of the loads caused by strip tension $T_\sigma(\theta)$, strip weight $T_s(\theta)$ and looper weight $T_L(\theta)$:

$$T_{load}(\theta) = T_\sigma(\theta) + T_s(\theta) + T_L(\theta)$$

where $T_\sigma(\theta) = \sigma h w R_l \left[\sin(\theta+\beta) - \sin(\theta-\alpha)\right]$, $T_L(\theta) = gM_L R_G \cos\theta$ and $T_s(\theta) \approx 0.5 g \rho L h w R_l \cos\theta$.

2.2. Tension Dynamics

Interstand strip tension is defined by the strip stretch and Young's modulus E of the strip:

$$\sigma(t) = E\left[\frac{L'(\theta) - (L + \xi(t))}{L + \xi(t)}\right] \tag{2}$$

for $L'(\theta) > (L + \xi(t))$ where θ is the looper angle; L is the interstand length; $L'(\theta)$ is the geometric looper length between stands; $L + \xi(t)$ is the accumulated material length which changes due to the mass flow difference of the strip between stands. $L'(\theta)$ is evaluated as follows (see Figure 1):

$$L'(\theta) = l_1(\theta) + l_2(\theta)$$

$$l_1(\theta) = \sqrt{(L_1 + R_l\cos\theta)^2 + (R_l\sin\theta + R_r - H_1)^2}$$

$$l_2(\theta) = \sqrt{(L_4 - R_l\cos\theta)^2 + (R_l\sin\theta + R_r - H_1)^2}$$

and $\xi(t)$ is evaluated as follows:

$\dot{\xi}(t) = v_s^i(t) - V_s^{i+1}(t) + w_\xi(t)$ and $v_s^i(t) - V_s^{i+1}(t) = \left(1 + S_f^i\right)V_R^i(t) - \left(1 - S_b^{i+1}\right)V_R^{i+1}(t)$

where $v_s^i(t)$, the strip speed leaving the upstream stand i, depends on the stand speed $V_R^i(t)$ and the forward slip S_f^i which occurs between the work rolls and the strip; $V_s^{i+1}(t)$, the strip speed entering the downstream stand $i+1$, depends on the stand speed $V_R^{i+1}(t)$ and the backward slip S_b^{i+1}; $w_\xi(t)$ represents unmodeled perturbations; S_f^i and S_b^{i+1} are sensitive to the tension σ and are evaluated as follows:

$$S_f^i = \frac{R_W^i}{h_i}(\gamma_i)^2 \quad \text{and} \quad S_b^{i+1} = 1 - \frac{h_{i+1}}{h_i}(1 + S_f^{i+1})$$

where $\gamma_i = \sqrt{\frac{h_i}{R_W^i}} \tan\left[\frac{1}{2}\arctan\sqrt{\frac{\varepsilon_i}{1-\varepsilon_i}} + \frac{\pi}{8}\ln(1-\varepsilon_i)\sqrt{\frac{h_i}{R_W^i}} + \frac{1}{2}\sqrt{\frac{h_i}{R_W^i}}\left(\frac{\sigma_i}{K} - \frac{\sigma_{i-1}}{K}\right)\right]$, $\varepsilon_i = \frac{h_{i-1} - h_i}{h_{i-1}}$. σ_i represents the strip tension between stand i and stand $i+1$ while σ_{i-1} for the strip tension between stand $i-1$ and stand i. h_{i-1}, h_i and h_{i+1} represent strip exit thickness of stand $i-1$, i and $i+1$ respectively. K denotes the steel deformation resistance. As far as the i th looper is concerned, for the sake of simplicity, we have $\sigma_i = \sigma$, $h_i = h$ and assume that σ_{i-1}, σ_{i+1}, $V_R^{i+1}(t)$ are invariant. Interested readers may refer to [13] for more information.

It is necessary to point out that $\xi(t)$ in (2) is rather small compared with L. As a result, $L + \xi(t)$ can be approximated by L. However, $\xi(t)$ can't be ignored in the numerator of (2) because $L'(\theta) - L$ and $\xi(t)$ are of the same order of magnitude. So the derivative of $\sigma(t)$ is

$$\begin{aligned}\dot{\sigma}(t) &= \frac{E}{L}\left[\frac{d}{dt}L'(\theta) - \dot{\xi}(t)\right] \\ &= \frac{E}{L}\left[R_l\left[\sin(\theta+\beta) - \sin(\theta-\alpha)\right]\dot{\theta}(t) - \left(\left(1+S_f^i\right)V_R^i(t) - \left(1-S_b^{i+1}\right)V_R^{i+1} + w_{\xi}(t)\right)\right]\end{aligned} \tag{3}$$

where α and β (upstream/downstream strip angle) are evaluated as $\alpha = \tan^{-1}\left[\left(R_l\sin\theta - H_1 + R_r\right)/\left(L_1 + R_l\cos\theta\right)\right]$ and $\beta = \tan^{-1}\left[\left(R_l\sin\theta - H_1 + R_r\right)/\left(L_4 - R_l\cos\theta\right)\right]$.

Table 1. Nomenclature

Symbol	Quantity
θ	looper angle
ω	looper angular speed
σ	strip tension
R_l	looper arm length
h	strip exit thickness
H	strip entry thickness
w	strip width
R_W^i	work roll radius of the i th stand
R_W^{i+1}	work roll radius of the $i+1$ th stand
M_L	looper mass
R_G	distance between pivoting point of the looper and center of gravity of the looper
R_r	radius of the looper roll
L	distance between two stands
L_1	distance between the i th stand and the looper pivot
L_4	distance between the looper pivot and the $i+1$ th stand
ρ	steel density
$l_1(\theta)$	distance between the i th stand and the looper roll
$l_2(\theta)$	distance between the looper roll and the $i+1$ th stand
$\xi(t)$	deviation of the interstand strip length with respect to L
g	gravitational constant
H_1	distance between actual pass line and looper pivot

2.3. Actuator Dynamics

As for the actuators, they are actually based on pre-existing basic controllers: the looper actuator torque $T_u(t)$ is controlled by ATR (automatic torque regulator) and the stand work roll speed $V_R^i(t)$ is controlled by ASR (automatic speed regulator). They are subject to dynamics which are not negligible and can be modeled as first-order transfer functions with time constants T_{ATR} and T_{ASR} respectively.

$$\dot{T}_u(t) = -\frac{1}{T_{ATR}}T_u(t) + \frac{1}{T_{ATR}}T_u^{ref}(t) + \frac{1}{T_{ATR}}e_t \tag{4a}$$

$$\dot{V}_R^i(t) = -\frac{1}{T_{ASR}}V_R^i + \frac{1}{T_{ASR}}V_R^{i,ref}(t) + \frac{1}{T_{ASR}}e_v \tag{4b}$$

where $T_u^{ref}(t)$ and $V_R^{i,ref}(t)$ are the references of $T_u(t)$ and $V_R^i(t)$ respectively. e_t and e_v are unmodeled dynamics and disturbances.

2.4. Approximately Linearized State Space Model

From the tension, looper and actuator dynamic equations presented above, the overall system can be described by the following nonlinear state model:

$$\begin{cases} \dot{\theta}(t) = \omega(t) \\ \dot{\omega}(t) = \frac{1}{J}\left(T_u(t) - \left(T_\sigma(\theta) + T_s(\theta) + T_L(\theta)\right) + w_\omega(t)\right) \\ \dot{\sigma}(t) = \frac{E}{L}\left[F_3(\theta)\omega(t) - \left(\left(1+S_f^i\right)V_R^i(t) - \left(1-S_b^{i+1}\right)V_R^{i+1} + w_\xi(t)\right)\right] \\ \dot{T}_u(t) = -\frac{1}{T_{ATR}}T_u(t) + \frac{1}{T_{ATR}}T_u^{ref}(t) + \frac{1}{T_{ATR}}e_t \\ \dot{V}_R^i(t) = -\frac{1}{T_{ASR}}V_R^i + \frac{1}{T_{ASR}}V_R^{i,ref}(t) + \frac{1}{T_{ASR}}e_v \end{cases} \tag{5}$$

where $F_3(\theta) = R_l\left[\sin(\theta+\beta) - \sin(\theta-\alpha)\right]$ for clarity and simplicity. The control problem is to design control signals $V_R^{i,ref}(t)$ and $T_u^{ref}(t)$ so that the looper angle $\theta(t)$ and the strip tension $\sigma(t)$ track the reference values θ_r and σ_r respectively as exactly as possible.

Since the full nonlinear model given in (5) is not suitable for controller design, we approximately linearize the model (by Taylor's series) about the output references θ_r and σ_r of the system which could be expressed by

$$\begin{bmatrix} \dot{\Delta\theta} \\ \dot{\Delta\omega} \\ \dot{\Delta\sigma} \\ \dot{\Delta T_u} \\ \dot{\Delta V_R^i} \end{bmatrix} = \begin{bmatrix} 0 & 1 & 0 & 0 & 0 \\ -\frac{1}{J}\left(\frac{\partial T_{load}}{\partial\theta}\right) & 0 & -\frac{1}{J}\left(\frac{\partial T_\sigma}{\partial\sigma}\right) & \frac{1}{J} & 0 \\ 0 & \frac{E}{L}F_3(\theta) & -\frac{E}{L}\left(\frac{\partial S_f^i}{\partial\sigma}V_R^i + \frac{\partial S_b^{i+1}}{\partial\sigma}V_R^{i+1}\right) & 0 & -\frac{E}{L}\left(1+S_f^i\right) \\ 0 & 0 & 0 & -\frac{1}{T_{ATR}} & 0 \\ 0 & 0 & 0 & 0 & -\frac{1}{T_{ASR}} \end{bmatrix} \begin{bmatrix} \Delta\theta \\ \Delta\omega \\ \Delta\sigma \\ \Delta T_u \\ \Delta V_R^i \end{bmatrix} + \begin{bmatrix} 0 & 0 \\ 0 & 0 \\ 0 & 0 \\ \frac{1}{T_{ATR}} & 0 \\ 0 & \frac{1}{T_{ASR}} \end{bmatrix} \begin{bmatrix} \Delta T_u^{ref} \\ \Delta V_R^{i,ref} \end{bmatrix} + \begin{bmatrix} 0 \\ \frac{1}{J}w_\omega \\ \frac{E}{L}w_\xi \\ \frac{1}{T_{ATR}}e_t \\ \frac{1}{T_{ASR}}e_v \end{bmatrix} \tag{6}$$

In order to eliminate the steady state error, we induce two state variables representing the integral of the output

$$\begin{cases} \dot{\Delta q} = \Delta\theta \\ \dot{\Delta p} = \Delta\sigma \end{cases}. \tag{7}$$

And the block diagram of the linearized model is given in Figure 2.

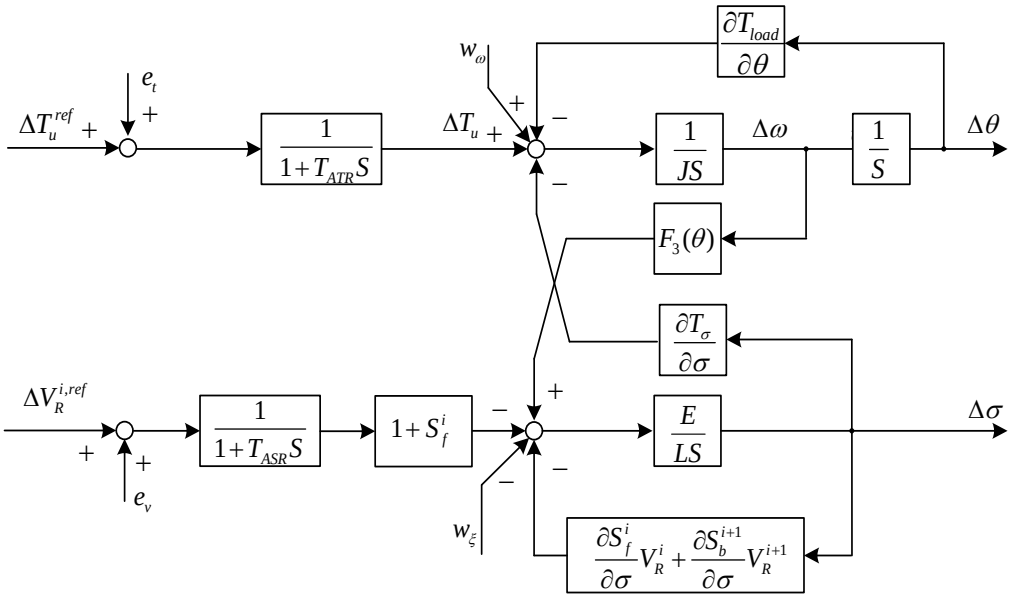

Figure 2. Block Diagram of the Linearized Looper-Tension System

2.5. Disturbances and Unmodeled Dynamics

There are disturbances and unmodeled dynamics from several sources which affect the looper and tension system.

For the tension loop, the main disturbance comes from the mass flow change. The change is mainly caused by the fast action of AGC systems in the case of temperature variations, roll eccentricity, thickness variations of the strip and so on. Strip temperature variations are mainly caused by skid marks, which are usually of periodic nature and occur at low frequencies. And roll eccentricity is a general term implying the out-of-roundness of backup and work rolls. Since roll rotation speeds are precisely known, eccentricity effects can easily be detected in spectral analysis of the real plant data. This disturbance is at higher frequencies. Another speed disturbance source is the set-up mismatch at the mills which creates a constant disturbance. Besides, the forward slip and backward slip, which are influenced by the time varying tension, are uncertain. So a 5% speed error of the nominal strip speed is frequently encountered. Among all the speed disturbances, the strip temperature and roll eccentricity are the major disturbances, whose magnitude can be estimated by the stand model provided in [4]. And these two kinds of disturbances will be used in the simulation to evaluate the proposed algorithm.

For the angle loop, disturbances and unmodeled dynamics come from the vicious friction phenomena of the hydraulic cylinder, the torque on the looper to bend the strip and so on. These disturbances and unmodeled dynamics are absorbed in $w_\omega(t)$. However, $w_\omega(t)$ is relatively small compared with $w_\xi(t)$. The speed perturbation $w_\xi(t)$ is the main source of disturbance.

For the actuators, the pre-existing basic controllers (ATR and ASR) are extremely complicated. Disturbances and unmodeled dynamics are mainly from the first-order approximation of the actuator dynamics. This part of disturbances (absorbed in e_t and e_v) are neglected in most existing works, which might deteriorate the performance of the proposed schemes. Therefore, we counteract these matched disturbances by ISMC technique to make the control strategy more reliable.

3. Review of ISMC and H∞ Technique

For the sake of the readers' convenience, a brief introduction of ISMC and H∞ technique is given in this section. And the specific combination of these two techniques is explained thoroughly.

3.1. Integral Sliding Mode Control

For the sake of completeness and the readers' conveniences, we consider a disturbed controllable linear system

$$\dot{x} = Ax + Bu + \phi \tag{8}$$

of the following regular form:

$$\begin{bmatrix} \dot{x}_1 \\ \dot{x}_2 \end{bmatrix} = \begin{bmatrix} A_{11} & A_{12} \\ A_{21} & A_{22} \end{bmatrix} \begin{bmatrix} x_1 \\ x_2 \end{bmatrix} + \begin{bmatrix} 0 \\ B_1 \end{bmatrix} u + \begin{bmatrix} D_{11} \\ 0 \end{bmatrix} \phi_1 + \begin{bmatrix} 0 \\ D_{22} \end{bmatrix} \phi_2 \tag{9}$$

where $x_1 \in \mathrm{R}^{n-m}$, $x_2 \in \mathrm{R}^m$, $x = \begin{bmatrix} x_1 \\ x_2 \end{bmatrix} \in \mathrm{R}^n$ is the state vector, and $A = \begin{bmatrix} A_{11} & A_{12} \\ A_{21} & A_{22} \end{bmatrix} \in \mathrm{R}^{n \times n}$ is the system matrix; $u \in \mathrm{R}^m$ is the control input vector with the gain matrix $B = \begin{bmatrix} 0 \\ B_1 \end{bmatrix} \in \mathrm{R}^{n \times m}$, and $B_1 \in \mathrm{R}^{m \times m}$ is of full rank; $\phi = \begin{bmatrix} D_{11} \\ 0 \end{bmatrix} \phi_1 + \begin{bmatrix} 0 \\ D_{22} \end{bmatrix} \phi_2$, $\phi_1 \in \mathrm{R}^p$, $\phi_2 \in \mathrm{R}^q$ represent bounded disturbances caused by parameter variations and external perturbations, and $D_{11} \in \mathrm{R}^{(n-m) \times p}$, $D_{22} \in \mathrm{R}^{m \times q}$ are corresponding disturbance gain matrices respectively.

As we can see from the regular form given in (9): $\phi_2 \in \mathrm{R}^q$ act on the control input channel (known as matched disturbances); $\phi_1 \in \mathrm{R}^p$, which enter the state equation at points that different from the control inputs, are treated as unmatched ones; and $\phi_1 \in \mathrm{R}^p$, $\phi_2 \in \mathrm{R}^q$ are clearly separated in the regular form. Such a structure for the system is quite common in real world applications, especially for systems whose actuators are subject to unmodelled dynamics, perturbations, parameter variations and so on. And the approximately linearized loop-tension dynamic system (6)-(7) investigated in this paper would be a good example for this regular form.

In order to overcome the shortages of the conventional SMC (the lack of robustness against unmatched disturbances, the reaching phase and so on), ISMC is proposed, which is regarded as a way to combine the use of conventional SMC with that of so-called "high level controller". The high level controller is designed to robustly stabilize the nominal system with unmatched disturbances, while ISMC rejects the matched disturbances. The basic idea is to design the control law as the combination of two parts:

$$u(x,t) = u_0(x,t) + u_1(x,t) \tag{10}$$

where the continuous nominal part $u_0(x,t)$ is responsible for the performance of the nominal system; and the discontinuous part $u_1(x,t)$ is constructed by ISMC. The latter part penalizes the difference between the actual and the nominal trajectories by ensuring the sliding motion, and the corresponding sliding manifold is defined by $\{x | s(x,t) = 0\}$ where $s(x,t)$ represents the trajectory difference (projected along a given matrix G):

$$s(x,t) = G\left[x(t) - x(t_0) - \int_{t_0}^{t} \left(Ax(\tau) + Bu_0(x,\tau) \right) d\tau \right] \tag{11}$$

Unlike the conventional SMC, we have $s(x,t_0) = 0$, that is, the ISMC system will always start at the manifold (eliminating the reaching phase problem). The discontinuous control $u_1(x,t)$, which enforces the sliding motion, is usually selected as

$$u_1(x,t) = -\rho(x,t) \frac{(GB)^T s(x,t)}{\left\| (GB)^T s(x,t) \right\|}. \tag{12}$$

From now on, we will omit some of the functions' arguments for the sake of convenience. And the motion equations of (8) at the sliding manifold can be determined

by the equivalent control method, that is, solving the equation $\dot{s}=0$:

$$\dot{s}=G\left[Ax+B(u_0+u_1)+\phi-\left(Ax+Bu_0\right)\right]=G\left[Bu_1+\phi\right]=0 \tag{13}$$

Under the assumption that GB is invertible, the equivalent control is given as

$$u_{1eq}=-(GB)^{-1}G\phi. \tag{14}$$

By substituting u_{1eq} for u_1 in (10), we have the sliding dynamic

$$\dot{x}_{eq}=Ax_{eq}+Bu_0+\phi_{eq},\quad \phi_{eq}=\left(I-B(GB)^{-1}G\right)\phi. \tag{15}$$

The remaining problem will be the selection of matrix G, such that, the equivalent disturbance ϕ_{eq} is minimal which guarantees better disturbance attenuation performance of (15) under the nominal control u_0. This problem is thoroughly discussed in [10], and $G=B^{+}=\left(B^TB\right)^{-1}B^T$ (the left inverse of B) is a suitable choice. We have $u_1=-\rho s/\|s\|$ by substitute $G=B^{+}$ into (12). As for the choice of ρ, which enforces the sliding motion, there is not much difference from the conventional SMC technique. That is, consider the candidate Lyapunov function $V=s^Ts/2$, ρ should be chosen high enough to ensure the negativity of $\dot{V}$:

$$\begin{aligned}
&\dot{V}=s^T\dot{s}\\
&=s^TG\left[Bu_1+\phi\right]\\
&=s^T\left[u_1+B^{+}\phi\right]\\
&=s^T\left[-\rho\frac{s}{\|s\|}+B^{+}\phi\right].\\
&=-\rho\|s\|+s^TB^{+}\phi\\
&\le-\rho\|s\|+\|s\|\|B^{+}\phi\|\\
&\le-\|s\|\left(\rho-\|B^{+}\phi\|\right)
\end{aligned} \tag{16}$$

So we have $\dot{V}<0$ if $\rho>\|B^{+}\phi\|$. For the system in regular form (9), the equivalent dynamic of the closed loop system will be

$$\dot{x}_{eq}=\left[\begin{array}{c:c}A_{11} & A_{12}\\ \hdashline A_{21} & A_{22}\end{array}\right]x_{eq}+\left[\begin{array}{c}0\\ \hdashline B_1\end{array}\right]u_0+\left[\begin{array}{c}D_{11}\\ \hdashline 0\end{array}\right]\phi_1. \tag{17}$$

As a result, the evolution of the states was the same as that attained by applying the high level controller to the system with only unmatched disturbances (without matched ones), which makes the control strategy more reliable. And due to the minimization of equivalent disturbance ϕ_{eq}, the ISMC method will result in better disturbance attenuation performance (interested readers may refer to [10] for more information).

3.2. H∞ Control

Since the ISMC technique introduced above will force the system (perturbed by matched disturbances) follow the evolution of (17), the nominal control u_0 could be designed by another robust method based on (17). This specific combination will compensate a well-known drawback of SMC, *i.e.*, the lack of robustness against unmatched disturbance. As we are considering the external disturbance attenuation problem of the loop-tension system (6)-(7), the linear H∞ control technique is chosen.

In the literature, the H∞ approach is regarded as one of the efficient tools to design optimal controllers for disturbance attenuation, which minimize the truncated L_2 gain from disturbance to an artificial penalty variable (the cost associated to the state and control). For the sake of completeness and the readers' conveniences, we revisit the background of H∞ control for linear systems of the form:

$$\dot{x}=Ax+Bu+Dw \tag{18}$$

$$z=Cx+Hu \tag{19}$$

where the state $x\in\mathbb{R}^n$, the control input $u\in\mathbb{R}^p$, the disturbance $w\in\mathbb{R}^m$, the cost associated to state and input $z\in\mathbb{R}^{n+p}$, and all the matrices are of appropriate dimension.

The goal is to design a state feedback controller $u = Kx$ which minimizes the H∞ norm of the transfer function T_{zw} (of the closed-loop system) that goes from w to z, *i.e.*,

$$\gamma^* = \min_K \sup_{w \in L_2 - \{0\}} \frac{\|z\|_{L_2}}{\|w\|_{L_2}} = \min_K \|T_{wz}(s)\|_\infty = \min_K \left\| (C + HK)\left[sI - (A + BK) \right]^{-1} D \right\|_\infty \quad (20)$$

where γ^* is the optimal performance index. This problem is solvable under the following typical assumption.

Assumption 1: (A, B) is stabilizable and (C, A) is detectable.

And the following lemma (given without proof, interested readers may refer to [14] for more information) is a standard result of H∞ control.

Lemma 1: Given Assumption 1, one such optimal controller stated in (20) can be chosen as

$$u = W^*(X^*)^{-1} x$$

where (ρ^*, X^*, W^*) is a optimal solution of the following optimal problem with LMI (Linear Matrix Inequality) constraints:

$$\min \rho$$

$$\text{s.t. (i)} \begin{bmatrix} AX + BW + (AX + BW)^T & D & (CX + HW)^T \\ D^T & -I & 0 \\ CX + HW & 0 & -\rho I \end{bmatrix} < 0,$$

$$\text{(ii)}\ X > 0$$

and corresponding optimal performance index $\gamma^* = \min_K \|T_{wz}(s)\|_\infty = \sqrt{\rho^*}$.

To summarize, for the regular form (9), the H∞ controller u_0 could be designed to attenuate the unmatched disturbance ϕ_1 regardless of the matched one ϕ_2. And the matched disturbance ϕ_2 will be further dealed by a discontinuous controller u_1 based on ISMC. With this specific combination, we could expect a more reliable system with better performances.

4. Looper and Tension Control Architecture

For the sake of comparison, three types of conventional PID control schemes are described in this section. And a new control architecture, based on the combination of H∞ and ISMC, and aimed at better performances, is introduced subsequently.

4.1. Conventional PID Control Schemes

There are mainly three kinds of conventional PID control schemes in industry.

The first PI control algorithm, which is applied when tension is not available, only detects looper position. Tension is controlled by varying the torque supplied to the looper using LTCB (looper torque calculation block). And looper angle is controlled by the speed of the upstream main drive motor. The second PID control algorithm shown in Figure 3, where T_0 and V_0 are the nominal reference variables of the control loops. This algorithm adds tension feedback to the system. Tension is controlled by a PI regulator which acts on the input of ASR. And looper angle is controlled by a PID regulator which acts on the input of ATR. And the last PID control algorithm works oppositely to the second one, that is, the control pairings is swapped: Tension is controlled by ATR, while looper angle is controlled by ASR.

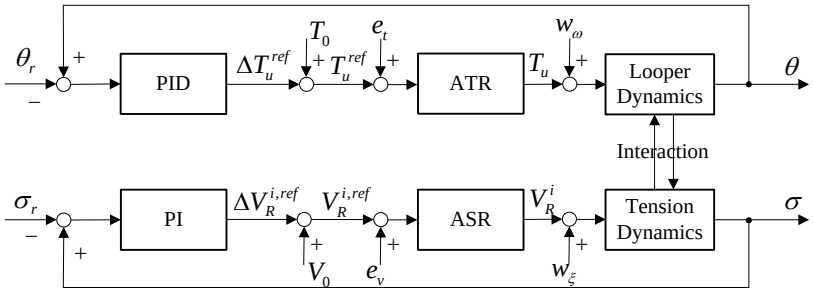

Figure 3. Conventional PID Control Architecture

Owing to their simplicity, the above conventional PID control techniques are common control methods in practice. However, these schemes result in slow responses and large deviations in both the tension and looper angle in presence of disturbances and unmodeled dynamics. Due to the nonlinear nature of the system, the conventional PID control schemes have an obvious problem that high gain causes instability whereas low gain gives poor performances. Hence, in order to overcome the shortages of the conventional PID schemes, we proposed an alternative robust H∞ control scheme based on ISMC.

4.2. Application of ISMC and H∞ Technique to Looper-Tension Control

In order to apply the ISMC and H∞ methodology, we need to express the looper-tension dynamics (6)-(7) in the form of (9). And for the sake of clarity and simplicity, we calculate the system model according to the values of the parameters given in Table 2 (obtained from the real plant).

Thus we have:

$$\begin{bmatrix} \Delta\dot{q} \\ \Delta\dot{\theta} \\ \Delta\dot{\omega} \\ \Delta\dot{p} \\ \Delta\dot{\sigma} \\ \hdashline \Delta\dot{T}_u \\ \Delta\dot{V}_R^i \end{bmatrix} = \left[\begin{array}{ccccccc} 0 & 1 & 0 & 0 & 0 & 0 & 0 \\ 0 & 0 & 1 & 0 & 0 & 0 & 0 \\ 0 & -97.3 & 0 & 0 & -153 & 332 & 0 \\ 0 & 0 & 0 & 0 & 1 & 0 & 0 \\ 0 & 0 & 1.52 & 0 & -3.27 & 0 & -21.7 \\ \hdashline 0 & 0 & 0 & 0 & 0 & -100 & 0 \\ 0 & 0 & 0 & 0 & 0 & 0 & -25 \end{array}\right] \begin{bmatrix} \Delta q \\ \Delta\theta \\ \Delta\omega \\ \Delta p \\ \Delta\sigma \\ \hdashline \Delta T_u \\ \Delta V_R^i \end{bmatrix} + \begin{bmatrix} 0 & 0 \\ 0 & 0 \\ 0 & 0 \\ 0 & 0 \\ 0 & 0 \\ \hdashline 100 & 0 \\ 0 & 25 \end{bmatrix} \begin{bmatrix} \Delta T_u^{ref}(t) \\ \Delta V_R^{i,ref}(t) \end{bmatrix} + \begin{bmatrix} 0 & 0 \\ 0 & 0 \\ 332 & 0 \\ 0 & 0 \\ 0 & 20.69 \\ \hdashline 0 & 0 \\ 0 & 0 \end{bmatrix} \begin{bmatrix} w_\omega(t) \\ w_\xi(t) \end{bmatrix} + \begin{bmatrix} 0 & 0 \\ 0 & 0 \\ 0 & 0 \\ 0 & 0 \\ 0 & 0 \\ \hdashline 100 & 0 \\ 0 & 25 \end{bmatrix} \begin{bmatrix} e_t(t) \\ e_v(t) \end{bmatrix} \quad (21)$$

where the matrices and vectors are divided by dashed lines according to (9) exactly, that is:

$$x_1 = \begin{bmatrix} \Delta q \\ \Delta\theta \\ \Delta\omega \\ \Delta p \\ \Delta\sigma \end{bmatrix}, \quad A_{11} = \begin{bmatrix} 0 & 1 & 0 & 0 & 0 \\ 0 & 0 & 1 & 0 & 0 \\ 0 & -97.3 & 0 & 0 & -153 \\ 0 & 0 & 0 & 0 & 1 \\ 0 & 0 & 1.52 & 0 & -3.27 \end{bmatrix}, \quad A_{12} = \begin{bmatrix} 0 & 0 \\ 0 & 0 \\ 332 & 0 \\ 0 & 0 \\ 0 & -21.7 \end{bmatrix}, \quad D_{11} = \begin{bmatrix} 0 & 0 \\ 0 & 0 \\ 332 & 0 \\ 0 & 0 \\ 0 & -20.69 \end{bmatrix},$$

$$x_2 = \begin{bmatrix} \Delta T_u \\ \Delta V_R^i \end{bmatrix}, \quad A_{11} = \begin{bmatrix} 0 & 0 & 0 & 0 & 0 \\ 0 & 0 & 0 & 0 & 0 \end{bmatrix}, \quad A_{22} = \begin{bmatrix} -100 & 0 \\ 0 & -25 \end{bmatrix}, \quad B_1 = \begin{bmatrix} 100 & 0 \\ 0 & 25 \end{bmatrix}, \quad D_{22} = \begin{bmatrix} 100 & 0 \\ 0 & 25 \end{bmatrix}. \quad (22)$$

Table 2. Parameters of the Looper and Tension System

Variable	Value	Unit	Variable	Value	Unit
θ_r	20	deg	R_G	0.194	m
σ_r	8	MPa	r	0.0925	m
R_1	0.611	m	E	12000	MPa
h_3	0.00908	m	w	1.5	m
h_4	0.00728	m	L	5.8	m
h_5	0.00547	m	L_1	2.34	m
R_W^i	0.4	m	L_4	3.46	m
R_W^{i+1}	0.4	m	ρ	7800	kg/m^3
V_R^i	6.058	m/s	T_{ASR}	0.04	s^{-1}
V_R^{i+1}	8.596	m/s	T_{ATR}	0.01	s^{-1}
S_f^i	0.05	p.u.	g	9.8	N/kg
S_b^{i+1}	0.2	p.u.	H_1	0.195	m
M_L	1862.9	kg	J	172.65	kgm^2

4.2.1. H∞ Controller Design

As we can see from the control architecture discussed in Section 3, the first step is to design the nominal controller u_0 based on the equivalent dynamic equation (15), and the parameters of corresponding matrices are given as:

$$\begin{bmatrix} \dot{\Delta q} \\ \dot{\Delta\theta} \\ \dot{\Delta\omega} \\ \dot{\Delta p} \\ \dot{\Delta\sigma} \\ \dot{\Delta T_u} \\ \dot{\Delta V_R^i} \end{bmatrix} = \left[\begin{array}{ccccc|cc} 0 & 1 & 0 & 0 & 0 & 0 & 0 \\ 0 & 0 & 1 & 0 & 0 & 0 & 0 \\ 0 & -97.3 & 0 & 0 & -153 & 332 & 0 \\ 0 & 0 & 0 & 0 & 1 & 0 & 0 \\ 0 & 0 & 1.52 & 0 & -3.27 & 0 & -21.7 \\ \hline 0 & 0 & 0 & 0 & 0 & -100 & 0 \\ 0 & 0 & 0 & 0 & 0 & 0 & -25 \end{array}\right] \begin{bmatrix} \Delta q \\ \Delta\theta \\ \Delta\omega \\ \Delta p \\ \Delta\sigma \\ \Delta T_u \\ \Delta V_R^i \end{bmatrix} + \left[\begin{array}{cc} 0 & 0 \\ 0 & 0 \\ 0 & 0 \\ 0 & 0 \\ 0 & 0 \\ \hline 100 & 0 \\ 0 & 25 \end{array}\right] \begin{bmatrix} \Delta T_u^{ref}(t) \\ \Delta V_R^{i,ref}(t) \end{bmatrix} + \left[\begin{array}{cc} 0 & 0 \\ 0 & 0 \\ 332 & 0 \\ 0 & 0 \\ 0 & 20.69 \\ \hline 0 & 0 \\ 0 & 0 \end{array}\right] \begin{bmatrix} w_\omega(t) \\ w_\xi(t) \end{bmatrix} \quad (23)$$

Follow the design procedure introduced in Section 3.2, once the system (23) is given, the H∞ controller will be solely determined by weight matrices C, H of the penalty variable z in (19). As for C and H, they are chosen according to the real system characteristics, the trade-off between the closed-loop system performance and the control inputs, the state variable constraints and so on. Here, we take

$$C = \begin{bmatrix} 0.1 & 0 & 0 & 0 & 0 & 0 & 0 \\ 0 & 0.2 & 0 & 0 & 0 & 0 & 0 \\ 0 & 0 & 0.1 & 0 & 0 & 0 & 0 \\ 0 & 0 & 0 & 0.1 & 0 & 0 & 0 \\ 0 & 0 & 0 & 0 & 0.2 & 0 & 0 \\ 0 & 0 & 0 & 0 & 0 & 5 & 0 \\ 0 & 0 & 0 & 0 & 0 & 0 & 5 \\ 0 & 0 & 0 & 0 & 0 & 0 & 0 \\ 0 & 0 & 0 & 0 & 0 & 0 & 0 \end{bmatrix}, \quad H = \begin{bmatrix} 0 & 0 \\ 0 & 0 \\ 0 & 0 \\ 0 & 0 \\ 0 & 0 \\ 0 & 0 \\ 0 & 0 \\ 5 & 0 \\ 0 & 5 \end{bmatrix}.$$

The H∞ controller will be determined by the solution of the optimal problem stated in Lemma 1:

$$u_0 = Kx = \begin{bmatrix} -0.82 & -0.02 & -0.05 & -1.21 & 0.11 & -0.78 & 0.02 \\ -0.13 & -0.03 & 0.01 & 0.08 & 0.25 & 0.01 & -0.81 \end{bmatrix} \begin{bmatrix} \Delta q \\ \Delta\theta \\ \Delta\omega \\ \Delta p \\ \Delta\sigma \\ \Delta T_u \\ \Delta V_R^i \end{bmatrix} \tag{24}$$

and corresponding optimal performance index $\gamma^* = 7.0729$.

4.2.2. ISMC Controller Design

Once the nominal controller u_0 is determined, the remaining task will be the chosen of sliding manifold

$$s(x) = B^+ \left[x(t) - x(t_0) - \int_{t_0}^{t} \left(Ax(\tau) + Bu_0(x(\tau)) \right) d\tau \right] = 0, \tag{25}$$

and the controller u_1 to enforce the sliding motion which is usually given by the continuous approximation of (12), that is,

$$u_1 = -\rho \frac{s}{\|s\| + \varepsilon} \tag{26}$$

where

$$\rho > \|B^+ \phi\| = \left\| B^+ \left(\begin{bmatrix} D_{11} \\ 0 \end{bmatrix} \begin{bmatrix} w_\omega \\ w_\xi \end{bmatrix} + \begin{bmatrix} 0 \\ D_{22} \end{bmatrix} \begin{bmatrix} e_t \\ e_v \end{bmatrix} \right) \right\| = \left\| \begin{bmatrix} e_t \\ e_v \end{bmatrix} \right\| = \sqrt{e_t^2 + e_v^2} \tag{27}$$

and the positive constant $\varepsilon > 0$ is chosen according to the trade-off between the undesirable chattering and the performance of the approximated control law (26). And the overall control architecture is given in Figure 4 where the H∞ controller $K = [k_1 \quad k_2]^T$ and the sliding surface $s = [s_1 \quad s_2]^T$.

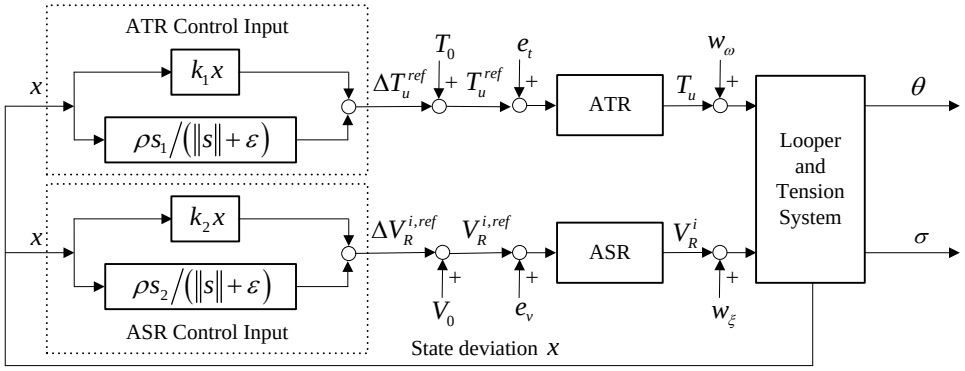

Figure 4. Sliding Mode Control Architecture

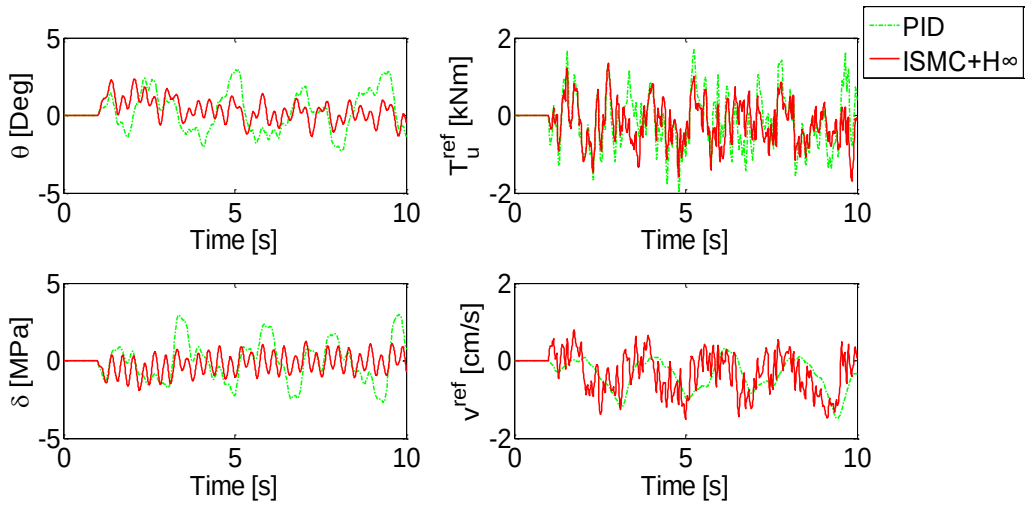

Figure 5. The Outputs and Inputs of the System in Presence of Sustaining Disturbances Active For $t > 1s$

5. Simulation results

Dynamic simulations using Matlab are carried out to evaluate the performances of the proposed H∞ controllers based on ISMC. The simulations are performed on a full nonlinear model tuned in agreement with the real plant and adequately grasp the dynamic behavior of the finishing mill. Therefore, they are very useful for tasks such as high performance control design and evaluation [15]. For the sake of comparison, we also report simulation results of the conventional PID algorithm given in Figure 3. And the PID regulators were developed by on-line tuning over many years.

The results reported are for Looper 4 in a seven-stand finishing mill. The looper angle reference θ_r is 20° and the strip tension reference σ_r is 8MPa. Simulation results are plotted in Figures 5-7, where red solid lines are the results for ISMC+ H∞ controllers, blue dashed dot lines for H∞ controllers and green dashed lines for PID controllers. Characteristic disturbances are included in the simulation analysis. Figures 5-6 present the outputs and inputs of the system in presence of the persisting disturbances

$w_\xi(t) = -0.4 - 0.4(\sin(10t+3) + \sin(7t))$ cm/s and $w_\omega(t) = 0.2\sin(20t)$ KNm

which are designed according to Section 2.5 and the characteristics of the real plant. And for the disturbances e_t and e_v in the actuators, since it's extremely difficult to model and estimate, we represent them by band-limited white noises with maximum 0.5 and minimum -0.5, which can easily be generated by the random source of Matlab Signal Processing Blockset. Consequently, the ISMC parameters are taken as $\rho = 1.2$ and $\varepsilon = 0.05$ according to Section 4.2.2. In general terms, the disturbances are more critical than the real case.

As indicated by the simulation results, the conventional PID controllers result in long settling time, and the deviations in both the tension and looper angle are greater than desired in presence of disturbances and unmodeled dynamics. In the case of the controllers proposed in this paper, the settling time and deviations due to the persisting disturbances are greatly reduced with respect to PID and H∞ controllers (Figures 5-6). As we can see from the control inputs that the ISMC technique may react quickly to the matched disturbances (even for the white noises). Actual values of the H∞ performance index for external disturbances (w_ω and w_ξ) are given in Figure 7. The index of the method proposed in this paper is slightly bigger than H∞ controllers, which is mainly caused by the energy consumed to overcome the internal disturbances (e_t and e_v). And

the proposed controllers achieve better dynamic performances with higher control efforts (the control input of ASR in Figures 5-6 especially).

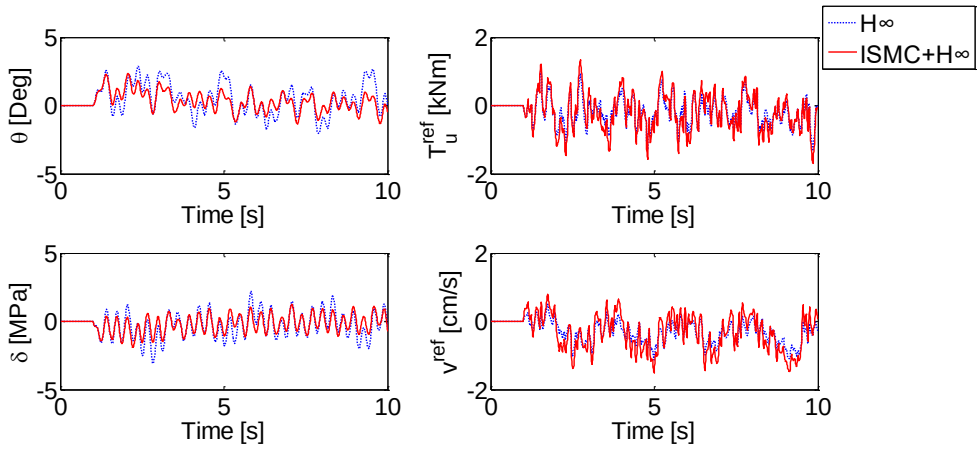

Figure 6. The Outputs And Inputs of the System In Presence of Sustaining Disturbances Active For $t>1s$

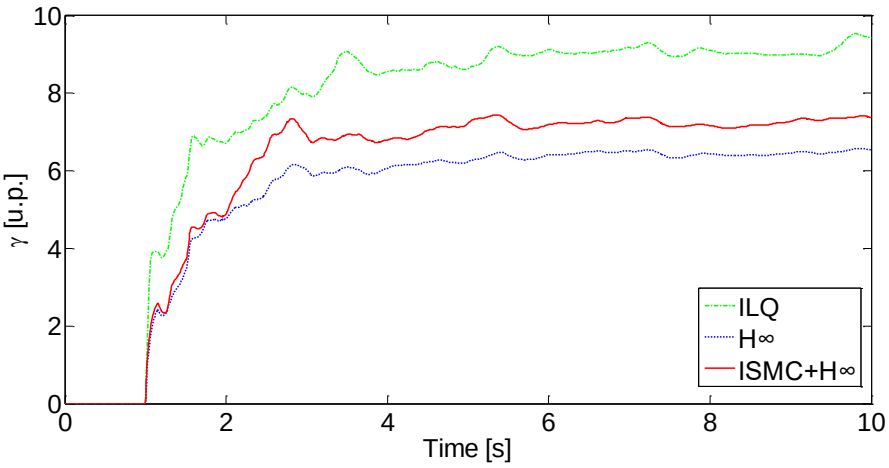

Figure 7. Actual Values of the H∞ Performance Index for External Disturbances Active From $t=1s$

6. Conclusion

An innovative looper and tension control approach based on the combination of H∞ and ISMC technique is investigated in this paper. By this particular combination, both matched and unmatched disturbances are attenuated better with respect to conventional PID and H∞ controllers.

And simulation results show the effectiveness of the proposed method which is more reliable.

However, since the stand and interstand are tightly coupled, future research efforts will be devoted to taking the interactions between the strip tension, strip thickness (gauge) and looper angle into account. Another research trend could be the extending of the proposed approach to the integral control problem consisting of seven stands and six loopers.

Acknowledgment

This work was partially supported by National Natural Science Foundation of China (61304095 & 61403254), Natural Science Foundation of Jiangsu Province (BK20130317), Jiangsu Planned Projects for Postdoctoral Research Funds (1302103B) and Suzhou Science and Technology Program (SGZ2013135).

References

[1] I. S. Choi, J. A. Rossiter and P. J. Fleming, "Looper and tension control in hot rolling mills: A survey", Journal of Process Control, vol. 17, no. 6, **(2007)**, pp. 509–521.
[2] L. P. Fan, M. Fang and Y. Liu, "Sliding mode control of strip rolling mill hydraulic AGC system", International Journal of Control and Automation, vol. 7, no. 8, **(2014)**, pp. 43–54.
[3] T. Hesketh, Y. A. Jiang, D. J. Clements, D. H. Butler and R. Laan, "Controller design for hot strip finishing mills", IEEE Transactions on Control System Technology, vol. 6, no. 2, **(1998)**, pp. 208–219.
[4] F. A. Cuzzola, "A multivariable and multi-objective approach for the control of hot-strip mills", Transactions of the ASME, vol. 128, no. 4, **(2006)**, pp. 856–868.
[5] G. Hearns, P. Reeve, P. Smith and T. Bilkhu, "Hot strip mill multivariable mass flow control", IEE Proceedings on Control Theory Applications, vol. 151, no. 4, **(2004)**, pp. 386–394.
[6] R. Furlan, F. A. Cuzzola and T. Parisini, "Friction compensation in the interstand looper of hot strip mills: A sliding-mode control approach", Control Engineering Practice, vol. 16, no. 2, **(2008)**, pp. 214–224.
[7] X. J. Sun and X. H. Feng, "Design and simulation of a new sliding mode controller for STATCOM based wind farm", International Journal of Control and Automation, vol. 7, no. 7, **(2014)**, pp. 46–64.
[8] H. Li and Y. Liu, "Study on sliding mode control with reaching law for DC motor", International Journal of Control and Automation, vol. 7, no. 5, **(2014)**, pp. 311–322.
[9] C. C. Wen and C. C. Cheng, "Design of sliding surface for mismatched uncertain systems to achieve asymptotical stability", Journal of Franklin Institute, vol. 345, no. 8, **(2008)**, pp. 926–941.
[10] H. H. Choi, "LMI-based sliding surface design for integral sliding mode control of mismatched uncertain systems", IEEE Transactions on Automatic Control, vol. 52, no. 4, **(2007)**, pp. 736–742.
[11] A. Estrada and L. M. Fridman, "Integral HOSM semiglobal controller for finite-time exact compensation of unmatched perturbations", IEEE Transactions on Automatic Control, vol. 55, no. 11, **(2010)**, pp. 2645–2649.
[12] W. Assawinchaichote, S. K. Nguang, P. Shi and E. K. Boukas, "H∞ fuzzy state-feedback control design for nonlinear systems with D-stability constraints: An LMI approach", Mathematics and Computers in Simulation, vol. 78, no. 4, **(2008)**, pp. 514–531.
[13] Y. K. Sun, "Model and control of strip tandem hot rolling", Metallurgy Industry Press, Beijing, China, **(2002)**.
[14] L. Yu, "Robust control: LMI approaches", Tsinghua University Press, Beijing, China, **(2002)**.
[15] S. K. Yildiz, J. F. Forbes, B. Huang, Y. Zhang, F. Wang, V. Vaculik and M. Dudzic, "Dynamic modelling and simulation of a hot strip finishing mill", Applied Mathematical Modelling, vol. 33, no. 7, **(2009)**, pp. 3208–3225.

Authors

Zhaozhun Zhong, he received the Ph.D. degree in automation from Shanghai Jiaotong University, Shanghai, China, in 2011.

He is currently a lecturer in Soochow University, Suzhou, China. His research interests include sliding mode control, robust control and control system simulation.

Jingcheng Wang, he received the Ph.D. degree in automation from Zhejiang University, Zhejiang, China, in 1998.

He is now a professor in Shanghai Jiaotong University, Shanghai, China. His research interests include robust control, intelligent control, real-time control and simulation.

Binna Song, she received the Ph.D. degree in Materials and Metallurgy from Northeastern University, Shenyang, China, in 2012.

She is currently a lecturer in Soochow University, Suzhou, China. Her research interests include porous metals, hot strip finishing mills and control system simulation.